BIOLOGY OF REPRODUCTION **82,** 136–145 (2010)
Published online before print 16 September 2009.
DOI 10.1095/biolreprod.109.079699

Phosphoglycerate Kinase 2 (PGK2) Is Essential for Sperm Function and Male Fertility in Mice[1]

Polina V. Danshina,[3,4] Christopher B. Geyer,[6] Qunsheng Dai,[6] Eugenia H. Goulding,[6] William D. Willis,[6] G. Barrie Kitto,[7] John R. McCarrey,[8] E.M. Eddy,[6] and Deborah A. O'Brien[2,3,4,5]

Laboratories for Reproductive Biology,[3] Department of Cell and Developmental Biology,[4] and Department of Pediatrics,[5] University of North Carolina School of Medicine, Chapel Hill, North Carolina
Laboratory of Reproductive and Developmental Toxicology,[6] National Institute of Environmental Health Sciences, National Institutes of Health, Research Triangle Park, North Carolina
Department of Chemistry and Biochemistry,[7] University of Texas at Austin, Austin, Texas
Department of Biology,[8] University of Texas at San Antonio, San Antonio, Texas

ABSTRACT

Phosphoglycerate kinase 2 (PGK2), an isozyme that catalyzes the first ATP-generating step in the glycolytic pathway, is encoded by an autosomal retrogene that is expressed only during spermatogenesis. It replaces the ubiquitously expressed phosphoglycerate kinase 1 (PGK1) isozyme following repression of *Pgk1* transcription by meiotic sex chromosome inactivation during meiotic prophase and by postmeiotic sex chromatin during spermiogenesis. The targeted disruption of *Pgk2* by homologous recombination eliminates PGK activity in sperm and severely impairs male fertility, but does not block spermatogenesis. Mating behavior, reproductive organ weights (testis, excurrent ducts, and seminal vesicles), testis histology, sperm counts, and sperm ultrastructure were indistinguishable between *Pgk2*$^{-/-}$ and wild-type mice. However, sperm motility and ATP levels were markedly reduced in males lacking PGK2. These defects in sperm function were slightly less severe than observed in males lacking glyceraldehyde-3-phosphate dehydrogenase, spermatogenic (GAPDHS), the isozyme that catalyzes the step preceding PGK2 in the sperm glycolytic pathway. Unlike *Gapdhs*$^{-/-}$ males, the *Pgk2*$^{-/-}$ males also sired occasional pups. Alternative pathways that bypass the PGK step of glycolysis exist. We determined that one of these bypass enzymes, acylphosphatase, is active in mouse sperm, perhaps contributing to phenotypic differences between mice lacking GAPDHS or PGK2. This study determined that PGK2 is not required for the completion of spermatogenesis, but is essential for sperm motility and male fertility. In addition to confirming the importance of the glycolytic pathway for sperm function, distinctive phenotypic characteristics of *Pgk2*$^{-/-}$ mice may provide further insights into the regulation of sperm metabolism.

gene targeting, glycolysis, male fertility, spermatogenesis, sperm metabolism, sperm motility

INTRODUCTION

Phosphoglycerate kinase (PGK) catalyzes the first ATP-generating step in the central metabolic pathway of glycolysis, converting 1,3-bisphosphoglycerate and ADP to 3-phosphoglycerate and ATP. There are two monomeric PGK isozymes in eutherian mammals that are encoded by distinct genes. The X-linked *Pgk1* gene is constitutively expressed in all cells that contain one or more active X chromosomes, including spermatogenic cells prior to entry into meiosis. *Pgk1* transcription is repressed in spermatocytes [1, 2] due to meiotic sex chromosome inactivation [3]. Effects of this inactivation are maintained by postmeiotic sex chromatin, and *Pgk1*, like most X-linked genes, remains transcriptionally silent throughout the haploid period of spermatogenesis [4]. *Pgk2*, an autosomal gene that evolved by retrotransposition from *Pgk1* [5, 6], is expressed exclusively during spermatogenesis [1, 7]. The temporal expression profile of *Pgk2* is opposite that of *Pgk1*, with *Pgk2* mRNA first appearing in preleptotene spermatocytes and increasing in pachytene spermatocytes and spermatids [1, 2].

Although *Pgk2* transcripts are present throughout meiotic prophase, PGK2 protein is found only in spermatids, indicating both transcriptional and translational control of expression. Most *Pgk2* mRNA is sequestered in translationally inactive ribonucleoproteins in spermatocytes, while a significant fraction is found on polysomes in round spermatids [8, 9]. Very low levels of PGK2 activity are first detected by isozyme gel electrophoresis at 22 days of age, when round spermatids begin to accumulate. PGK2 activity increases substantially in elongating spermatids and constitutes ~80% of the total PGK activity in the adult mouse testis [7, 10]. This increase in activity coincides with the initial immunohistochemical detection of PGK2 protein between steps 9 and 12 of spermiogenesis [11–13]. In contrast, both PGK1 activity and immunoreactivity are low in the adult testis, with highest levels in interstitial and Sertoli cells [10, 12].

Novel gene expression patterns during spermatogenesis modify glycolysis extensively, producing sperm with several glycolytic isozymes that have distinct structural and functional properties. In addition to *Pgk2*, glyceraldehyde-3-phosphate dehydrogenase, spermatogenic (*Gapdhs*); lactate dehydrogenase C (*Ldhc*); and two aldolase A (*Aldoa*)-related retrogenes (*Aldoart1* and *Aldoart2*) encode novel isozymes with restricted expression during spermatogenesis [14–18]. Alternative splicing generates other sperm isozymes, including hexokinase HK1S [19, 20] and ALDOA_V2 [18]. Unique features of these isozymes may be required for localization of the glycolytic

[1]Supported by National Institutes of Health (NIH) grants U01 HD45982 (D.A.O.) and R01 HD46637 (J.R.M.) from the Eunice Kennedy Shriver National Institute of Child Health and Human Development and the Intramural Research Program of the NIH, National Institute of Environmental Health Sciences (Z01 ES070076; E.M.E.).
[2]Correspondence: Deborah A. O'Brien, Department of Cell and Developmental Biology, CB# 7090, University of North Carolina School of Medicine, Chapel Hill, NC 27599-7090. FAX: 919 966 1856; e-mail: dao@med.unc.edu

Received: 13 July 2009.
First decision: 3 August 2009.
Accepted: 3 September 2009.

eISSN: 1529-7268 http://www.biolreprod.org
ISSN: 0006-3363

pathway in the principal piece of the sperm flagellum [21]. They may also contribute to enhanced stability, since these enzymes must remain functional until fertilization, or to altered regulation of energy metabolism, which may be required since glycolysis and oxidative phosphorylation are atypically compartmentalized in distinct segments of the highly polarized sperm flagellum.

In vitro studies of both mouse and human sperm indicate that glycolysis produces a significant fraction of the ATP in these cells [22–24] and is required for multiple steps in the fertilization cascade, including capacitation-dependent tyrosine phosphorylation [25, 26], hyperactivated motility, and penetration of the zona pellucida [24, 27–29]. In vivo gene targeting studies provide further evidence that glycolysis [30, 31], rather than mitochondrial metabolism [32], is essential for sperm motility and male fertility. *Gapdhs*$^{-/-}$ males are completely infertile and produce sperm that have very low ATP levels and exhibit no forward motility [30]. Fertility is also severely impaired in *Ldhc*$^{-/-}$ males, and sperm from these animals exhibit a temporal decline in motility and ATP levels [31].

Little, if any, PGK1 remains during the 14-day postmeiotic period of spermiogenesis in the mouse, and PGK2 is the only PGK isozyme detected by isozyme gel electrophoresis in sperm from the caput or cauda epididymis [33]. Like GAPDHS, PGK2 is positioned at a key transition point between the ATP-consuming and ATP-generating steps in the sperm glycolytic pathway. Unlike GAPDHS, however, PGK2 and LDHC are not tightly bound to the fibrous sheath, the cytoskeletal structure that defines the limits of the principal piece [15, 34]. In this study we eliminated PGK2 by gene targeting to determine if this isozyme is required for the completion of spermatogenesis and to further investigate the role of novel glycolytic enzymes in sperm structure and function.

MATERIALS AND METHODS

Generation of Pgk2$^{-/-}$ *Mice*

The *Pgk2* targeting vector was constructed using a modified pUCBM21 vector containing a *Pgk1* promoter-driven neomycin resistance (*Neo*) gene and the herpes simplex virus thymidine kinase (HSV-*tk*) gene for positive and negative selection, respectively. 129S6/SvEvTac genomic DNA fragments homologous to regions within the endogenous *Pgk2* locus on murine chromosome 17 were inserted into this backbone vector. The *Pgk2* 1.55-kb upstream homology arm was amplified by PCR and inserted into the *Hpa*I site of the vector, while the 4.02-kb downstream homology arm was isolated and introduced as a *Pme*I fragment from a genomic BAC clone containing *Pgk2* (clone 159H4; RPCI 22 BAC library) [35]. The complete sequence of the pUC*tk-Pgk2-Neo* knockout targeting vector was verified using BigDye v3.1 chemistry on an ABI Avant 3100 (Applied Biosystems, Foster City, CA). Transfection of *Not*I-linearized pUC*tk-Pgk2-Neo* DNA, screening of targeted TC-1 embryonic stem (ES) cells (gift of Philip Leder, Harvard Medical School, Boston, MA), and blastocyst injections were performed as described previously [36]. Homologous recombination resulted in the insertion of the *Neo* gene, replacing most of the *Pgk2* coding sequence (1059 bp; nt 21–1080 of GenBank sequence NM_031190) plus 40 bp upstream of the start codon (Fig. 1). Correctly targeted ES clones were identified by PCR using screening primers (5′-AGAGTAGGGCAGGAGGGAACATACAA-3′ in the 5′-flanking region of *Pgk2* and 5′-CCAGAAAGCGAAGGAGCAAAGC-3′ in the *Neo* gene). Clones were confirmed by Southern blot analysis (not shown) to distinguish *Eco*RV restriction fragments from the targeted (8.7 kb) and wild-type (WT; 13.3 kb) alleles using a 383-bp probe to a region upstream of the 5′-targeting arm.

Male chimeras from two ES cell lines (U32 and V8) were mated with C57BL/6NCrl females (Charles River Laboratories, Raleigh, NC), and germline transmission was confirmed by PCR screening. Heterozygous (*Pgk2*$^{+/-}$) offspring with a mixed genetic background (129S6/SvEvTac and C57BL/6NCrl) were mated to produce homozygous knockout (*Pgk2*$^{-/-}$), *Pgk2*$^{+/-}$, and WT (*Pgk2*$^{+/+}$) males for comparative analysis of fertility and sperm function. Genotypes of the mice were determined by PCR using a common reverse primer (5′-CATTTGGCGCAGCAAGTAGCAGTA-3′) with forward primers specific for the WT allele (5′-TGCTGACCCTGCTAAAG

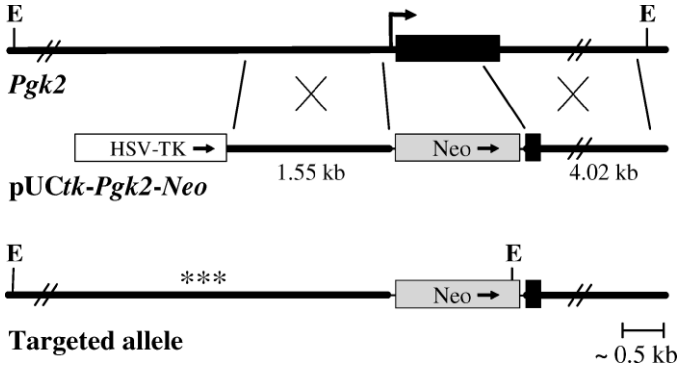

FIG. 1. Diagram of the *Pgk2* locus and gene targeting strategy. The intronless *Pgk2* coding sequence is shown as a black box, with the transcription start site indicated by a bent arrow. The targeting vector, pUC*tk-Pgk2-Neo*, contains a thymidine kinase cassette (HSV-TK) for negative selection and the neomycin resistance gene (Neo) for positive selection. Neo is flanked by 1.55-kb and 4.02-kb sequences homologous to regions that extend upstream and downstream from *Pgk2*. The targeted allele was created by homologous recombination to replace the majority of the *Pgk2* coding sequence with Neo. Restriction digestion with *Eco*RV (E) produces a 13.3-kb fragment from the endogenous gene and an 8.7-kb fragment from the targeted allele. Proper recombination was confirmed by Southern blotting using a probe (***) to a region upstream of the 5′-targeting arm.

TAGAAGC-3′) or a *Neo*-specific primer for the targeted allele (5′-ATGCCTGCTTGCCGAATATCATGG-3′). *Gapdhs*$^{-/-}$ mice [30] were also used to compare sperm ATP levels. Animal maintenance and experimental protocols were approved by the Institutional Animal Care and Use Committees of the University of North Carolina and The National Institute of Environmental Health Sciences.

Production of Rabbit Antisera to Recombinant Mouse PGK2

For expression of recombinant protein, the mouse *Pgk2* coding sequence was inserted into a modified p*beta*2MS plasmid designed to generate a C-terminal hexahistidine tag. This modified plasmid was transfected into BL21(DE3)pLysS *E. coli* (Stratagene, Cedar Creek, TX) by electroporation, and cells were grown overnight at 37°C in Luria broth medium supplemented with chloramphenicol and ampicillin. Cells were stored as glycerol stocks, and single colonies were grown to inoculate LB cultures for protein production. After inducing expression with isopropyl β-D-1-thiogalactopyranoside during the exponential growth phase and incubating the cultures for another 3 h, cells were harvested by centrifugation at 6000 × *g* at 4°C and stored at −80°C. Frozen cells (2 g) were suspended in 15 ml lysis buffer (50 mM NaH_2PO_4, 300 mM NaCl, and 10 mM imidazole; pH 8) and disrupted by sonication using a Vibra-cell Model VC40 (Sonics and Materials, Newton, CT) with the output control at 70 (three 30-sec periods with 30-sec intervals on ice between sonications). Debris was removed by centrifugation at 6000 × *g* for 30 min at 4°C. His-tagged mouse PGK2 was purified from the supernatant using Ni-NTA agarose affinity chromatography (Qiagen, Valencia, CA) according to the manufacturer's instructions. Eluted PGK2 was dialyzed against PBS at pH 7.0 to remove imidazole, and the sample was concentrated at 4°C using an Amicon Centriprep Ultracel YM-10 (Millipore, Bedford, MA) centrifuged at 1500 × *g*. His-tagged PGK2 was subjected to SDS-PAGE to evaluate purity and stored at −80°C.

Rabbit polyclonal antibodies against full-length mouse PGK2 with a C-terminal hexahistidine tag were prepared at the Virginia Harris Cockrell Cancer Research Center (The University of Texas M.D. Anderson Cancer Center Science Park, Bastrop, TX). Recombinant protein in complete Freunds adjuvant was used to immunize two rabbits, which were then boosted twice at 2-wk intervals with recombinant protein in incomplete Freunds adjuvant. Antiserum 517 was used for Western blotting and immunohistochemistry presented in this report.

Western Analysis and Immunohistochemistry

Standard Western blotting procedures were used to assess the specificity of antisera raised against mouse PGK2 and the effectiveness of our gene targeting

TABLE 1. *Pgk2*$^{-/-}$ and WT males have comparable reproductive organ weights and sperm counts.*

Genotype	Body weight (g)	Testis (mg)	Epididymis + vas (mg)	Seminal vesicles (mg)	Sperm count (10^6/cauda)
WT	36.2 ± 1.3	108 ± 4	56 ± 2	413 ± 19	25.7 ± 1.5
Pgk2$^{-/-}$	33.0 ± 2.0	117 ± 5	56 ± 2	377 ± 31	30.3 ± 2.5

*Values are means ± SEM. Seminal vesicles weights represent the combined weights of both glands, while others (testis, epididymis + vas deferens) are the weights of single organs (n = 17 for WT and n = 14 for *Pgk2*$^{-/-}$ mice for body and organ weights). The sperm counts represent the number collected from one cauda epididymis (n = 7 for each genotype). $P > 0.05$ for all comparisons between genotypes.

strategy. Total proteins from sperm and testes of WT and *Pgk2*$^{-/-}$ mice and somatic tissues of CD1 mice (Charles River Laboratories) were separated by SDS-PAGE on 10% polyacrylamide gels and transferred to Immobilon-P PVDF (polyvinylidene fluoride) membranes (Millipore, Bedford, MA) as described previously [18]. Protein concentrations were determined using the microassay procedure of the Bio-Rad Protein Assay (Bio-Rad, Hercules, CA). Western blotting was performed as described [18], substituting PBS-T (140 mM NaCl, 10 mM phosphate buffer, and 0.1 % Tween 20; pH 7.4) for TBS-T (140 mM NaCl, 3 mM KCl, 0.05% Tween-20, 25 mM Tris-HCl, pH 7.4). Membranes were incubated for 1 h at room temperature with the rabbit polyclonal antibody raised against PGK2 (1:7000), a rabbit polyclonal antibody specific for PGK1 (1:100 dilution; AP7094b; Abgent, San Diego, CA), or a mouse monoclonal antibody against α-tubulin (1:2000; T6199; Sigma-Aldrich, St. Louis, MO). After washing, the membranes were incubated for 45 min with affinity-purified goat anti-rabbit IgG or goat anti-mouse IgG + IgM conjugated to horseradish peroxidase (1:30 000; Kirkegaard & Perry Laboratories, Gaithersburg, MD). Immunoreactivity was detected with a chemiluminescent substrate for peroxidase (Amersham ECL; GE Healthcare Bio-Sciences, Piscataway, NJ).

Immunohistochemistry was performed using the avidin-biotin immunoperoxidase method (Vectastain ABC kit; Vector Laboratories, Burlingame, CA) according to the manufacturer's instructions. Testes were fixed in Bouin solution, dehydrated in a graded series of ethanol, and embedded in paraffin. Sections (8 μm) were deparaffinized prior to immunostaining. The same PGK2 antiserum used for Western blotting was used at a concentration of 1:2000 for these localization studies, and immune complexes were detected with 3,3′-diaminobenzidine tetrachloride (Sigma-Aldrich). Sections were counterstained with toluidine blue and photographed with a Spot RT Slider digital camera (Diagnostic Instruments, Sterling Heights, MD).

Analysis of Fertility, Sperm Production, and Sperm Ultrastructure

Male *Pgk2*$^{-/-}$ mice (2–4 mo old) were subjected to 3-mo mating trials to assess fertility. Each male was housed continuously with two females (C57BL/6NCrl or *Pgk*$^{+/-}$ females from the colony) that were replaced at 4- to 6-wk intervals and monitored for litters for 1 mo after being separated from males. Using this strategy, each male was tested with four to six females. Fertility of *Pgk2*$^{+/-}$ males was determined while mating them to maintain the colony. *Pgk2*$^{-/-}$ females were also mated individually with WT males for 2–5 mo to assess their fertility. For each test mating, the number, frequency, and size of litter were recorded.

As an initial assessment of the reproductive tract of *Pgk2*$^{-/-}$ males, the wet weights of testis, epididymis + vas deferens, and seminal vesicles were compared with WT males of the same age and genetic background. Sperm counts were also compared following collection from one cauda epididymis. Each cauda was clipped, and sperm were allowed to swim out into M16 medium (Specialty Media, Lavallette, NJ) for 15 min at 37°C in an incubator with 5% CO_2 in air, followed by extrusion of remaining sperm with fine forceps. Energy substrates in M16 medium include 5.55 mM glucose, 22 mM sodium lactate, and 0.55 mM sodium pyruvate. Sperm were diluted with H_2O to block motility and counted with a hemocytometer.

Testis histology was assessed on paraffin sections following fixation in Bouin solution. Sections were stained with periodic acid-Schiff and counterstained with hematoxylin [37] to facilitate staging of the seminiferous tubules [38]. Photomicrographs were taken with a Spot RT Slider digital camera.

Sperm ultrastructure was examined by scanning and transmission electron microscopy as described previously [30, 39]. For these analyses, images of sperm from two WT and two *Pgk2*$^{-/-}$ mice were recorded by an investigator who did not know the genotypes of the mice.

Sperm Enzyme Assays

Sperm were collected from each cauda epididymis in 0.5 ml M16 medium by carefully isolating and rinsing each cauda epididymis, gently clipping with iris scissors, and allowing sperm to swim out for 10 min at 37°C in an incubator with 5% CO_2 in air. Care was taken to minimize contamination with epithelial cells and erythrocytes. After washing in PBS, sperm lysates were prepared by sonication (3 × 2-sec pulses) using a Branson Sonifier 250 (Branson Ultrasonics Corporation, Danbury, CT) at 15–20 watts. Triplicate aliquots ($0.25–1 \times 10^6$ sperm) from each lysate were used for assaying PGK2 or acylphosphatase activity.

PGK activity was measured in the reverse reaction coupled with GAPDH, and the oxidation of NADH was monitored at 340 nm [40]. The reaction was started by adding sperm lysate to 400 μl of reaction mixture containing 10 mM 3-phosphoglycerate, 8 U/ml GAPDH, 2 mM ATP, 0.22 mM NADH, 10 mM $MgSO_4$, 2 mM dithiothreitol, and 30 mM HEPES (pH 7.5). One unit of activity was defined as the amount of enzyme that catalyses the oxidation of 1 μM NADH in 1 min.

Acylphosphatase activity was determined using a continuous optical method based on the difference in absorbance at 283 nm between benzoyl phosphate and benzoate at 25°C [41]. The benzoyl phosphate substrate was synthesized as previously described [42]. The reaction was initiated by adding sperm lysate to 400 μl of reaction mixture containing 5 mM benzoylphosphate and 1 M sodium acetate buffer (pH 5.3). One unit of activity is defined as the amount of enzyme that liberates 1 μmol of benzoate per min.

Sperm Motility

For analysis of motility, sperm were isolated as described for enzyme assays and incubated for 90 min under capacitating conditions in M16 medium at 37°C in an incubator with 5% CO_2 in air. Real-time videos were recorded immediately after isolation and at 90 min using a Leica DM IRB inverted microscope (40× objective; Leica Microsystems, Bannockburn, IL) equipped with Nomarski differential interference contrast optics (Leica). Quantitative parameters of sperm motility were monitored in 80 μm-depth 2X-CEL chambers (Hamilton Thorne Biosciences, Beverly, MA) and recorded (60 Hz) at 30-min intervals by computer-assisted sperm analysis (CASA) using an HTM-IVOS sperm analysis system (v12; Hamilton Thorne Biosciences). Sperm tracks (60 frames, 1 sec) and kinetic parameters were recorded for individual sperm, along with mean values from tracks with ≥30 points for average path velocity (VAP; μm/sec), straight line velocity (VSL; μm/sec), curvilinear velocity (VCL; μm/sec), amplitude of lateral head displacement (ALH; μm), beat cross frequency (BCF; Hz), straightness (STR; VSL/VAP × 100) and linearity (LIN; VSL/VCL × 100). Sperm with VAP > 80 μm/sec and STR > 50% were considered progressive.

Sperm ATP Levels and Oxygen Consumption

To measure ATP levels, sperm were isolated as described for enzyme assays and incubated in M16 medium for 90 min at 37°C in an incubator with 5% CO_2 in air. Triplicate aliquots were removed immediately after collection from the cauda epididymis and at subsequent 30-min intervals. These aliquots were adjusted to $\sim 10^4$ sperm per 50 μl M16, and ATP levels were determined using a luciferase bioluminescence assay (ATP Bioluminescence Assay kit CLS II; Roche Applied Science, Indianapolis, IN) as described previously [30].

After collecting sperm in glucose-free M2 medium [30], oxygen consumption was measured in a multichannel chamber of a computerized analyzer equipped with an oxygen-sensitive mini-electrode calibrated to air-saturated medium [43]. Measurements of oxygen consumption by sperm were initiated by adding $2–3 \times 10^7$ sperm to the reaction chamber containing 1 ml of M2 medium at room temperature. Oxygen consumption for sperm with intact membranes was measured in the presence of 50 μM dinitrophenol (Sigma-

Aldrich). To measure maximal respiratory activity of intracellular mitochondria in the presence of excess substrate, we permeabilized sperm plasma membranes with digitonin (50 μg/ml; Calbiochem, San Diego, CA) and monitored changes in the rate of oxygen consumption in the presence of succinate (10 mM), ethylene glycol-bis(2-aminoethylether)-*N*,*N*,*N*′,*N*′-tetraacetic acid (EGTA, 2.5 mM), and added cytochrome c (0.5 μg/ml; Sigma-Aldrich) to compensate for potential losses during permeabilization [44]. The rate of oxygen consumption was calculated using the dissolved oxygen concentration of 0.237 μmoles O_2/ml at room temperature and expressed as nmoles O_2 min^{-1} $(10^8$ sperm$)^{-1}$.

Statistical Analysis

Mean values ± SEM were calculated for each quantitative parameter, and error bars in all figures represent SEMs. GraphPad Prism 4 (GraphPad Software, San Diego, CA) was used for statistical analysis. Two-tailed Student *t*-tests were performed to assess statistical significance between *Pgk2*$^{-/-}$ and WT organ weights and sperm counts (Table 1). All other data were analyzed using one-way ANOVA followed by Bonferroni's multiple-comparison test. Differences were considered significant at $P < 0.05$.

RESULTS

Gene Targeting Eliminates PGK2 in Testis and Sperm

Since *Pgk2* is an intronless retrogene with a transcribed region that is only 1530 bp in length (NM_031190), we used a targeting strategy that eliminated all but the final 194 bp of coding sequence (Fig. 1). As expected, Western blot analysis showed strong reactivity with PGK2 in WT sperm and testis but did not detect PGK2 protein in sperm or testis from *Pgk2*$^{-/-}$ males (Fig. 2A, 30 μg protein per lane). This result was confirmed with two additional rabbit antisera raised against either recombinant mouse PGK2 or a PGK2-specific peptide corresponding to amino acids 316–333 (not shown). Longer exposures of Western blots indicated that all three antisera had some cross-reactivity with PGK1, which has the same molecular weight of ~45 000 and is ubiquitously expressed in somatic tissues. PGK1 was detected in most tissues when the blot shown in Figure 2A (30-sec exposure) was exposed to film for 15 min (Fig. 2B), although immunoreactivity was very faint in lung and testis from *Pgk2*$^{-/-}$ mice and absent in PGK2-null sperm. Comparable protein loads were confirmed by Coomassie blue staining (not shown) and α-tubulin immunoreactivity on a parallel blot (Fig. 2C). When protein loads were increased to 100 μg/lane, PGK1 was detected with an isozyme-specific antibody (AP7094b; Abgent) in all somatic tissues and in testis from WT or *Pgk2*$^{-/-}$ mice, but not in sperm from mice of either genotype (Fig. 2D). In addition, total PGK activity was indistinguishable from background in sperm from *Pgk2*$^{-/-}$ males and was approximately half of WT levels in sperm from *Pgk2*$^{+/-}$ mice (Fig. 2E).

Male Fertility Is Severely Impaired in Pgk2$^{-/-}$ Mice

Pgk2$^{-/-}$ males exhibited normal mating behavior and produced copulatory plugs, but sired very few pups during 3-mo continuous mating trials with two females per male. Females were replaced at least once during the mating period, and similar results were obtained when males were mated with C57BL/6NCrl females (males [n = 6] mated with a total of 32 females) or with *Pgk2*$^{+/-}$ females from the colony (males [n = 2] mated with a total of eight females). Four of these *Pgk2*$^{-/-}$ males were infertile, three sired a single small litter with one to four pups each, and one sired two litters with three and six pups. Although the infertile males were derived from the V8 ES cell line and the males with low fertility were derived from the U32 ES cell line, subsequent functional analyses (sperm counts, motility, ATP levels, etc.) did not detect any differences between *Pgk2*$^{-/-}$ males from either cell line. As a

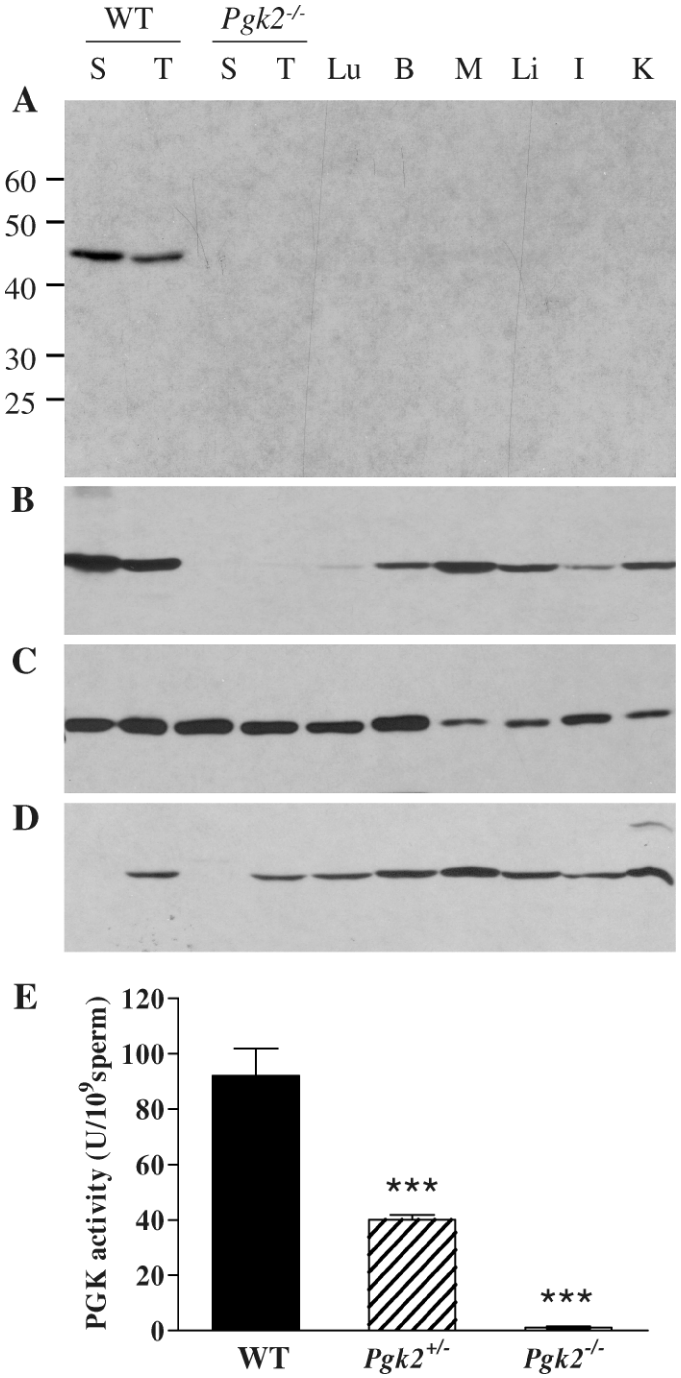

FIG. 2. Sperm from *Pgk2*$^{-/-}$ males lack PGK2 and PGK1. Western blot analysis was conducted to compare PGK isozymes in sperm (S) and testis (T) of *Pgk2*$^{-/-}$ mice with isozymes present in sperm and tissues from WT mice, including testis, lung (Lu), brain (B), skeletal muscle (M), liver (Li), intestine (I), and kidney (K). **A**) Blot containing protein from 0.5×10^6 sperm or 30 μg of tissue protein per lane was incubated with a PGK2 antibody (antiserum 517) and exposed to film for 30 sec after addition of a chemiluminescent substrate. **B**) The same blot shown in **A** was exposed to film for 15 min. **C**) Immunodetection of α-tubulin on a parallel blot (30 μg of protein per lane) confirmed protein integrity of these samples. **D**) Using an isozyme-specific antibody, PGK1 was detected in all tissues, but not in sperm, when protein loads were increased to 1×10^6 sperm or 100 μg of tissue protein per lane. **E**) Mean PGK activities ± SEM are shown for sperm from WT (n = 6), *Pgk2*$^{+/-}$ (n = 15), and *Pgk2*$^{-/-}$ (n = 5) mice. ***$P <$ 0.001.

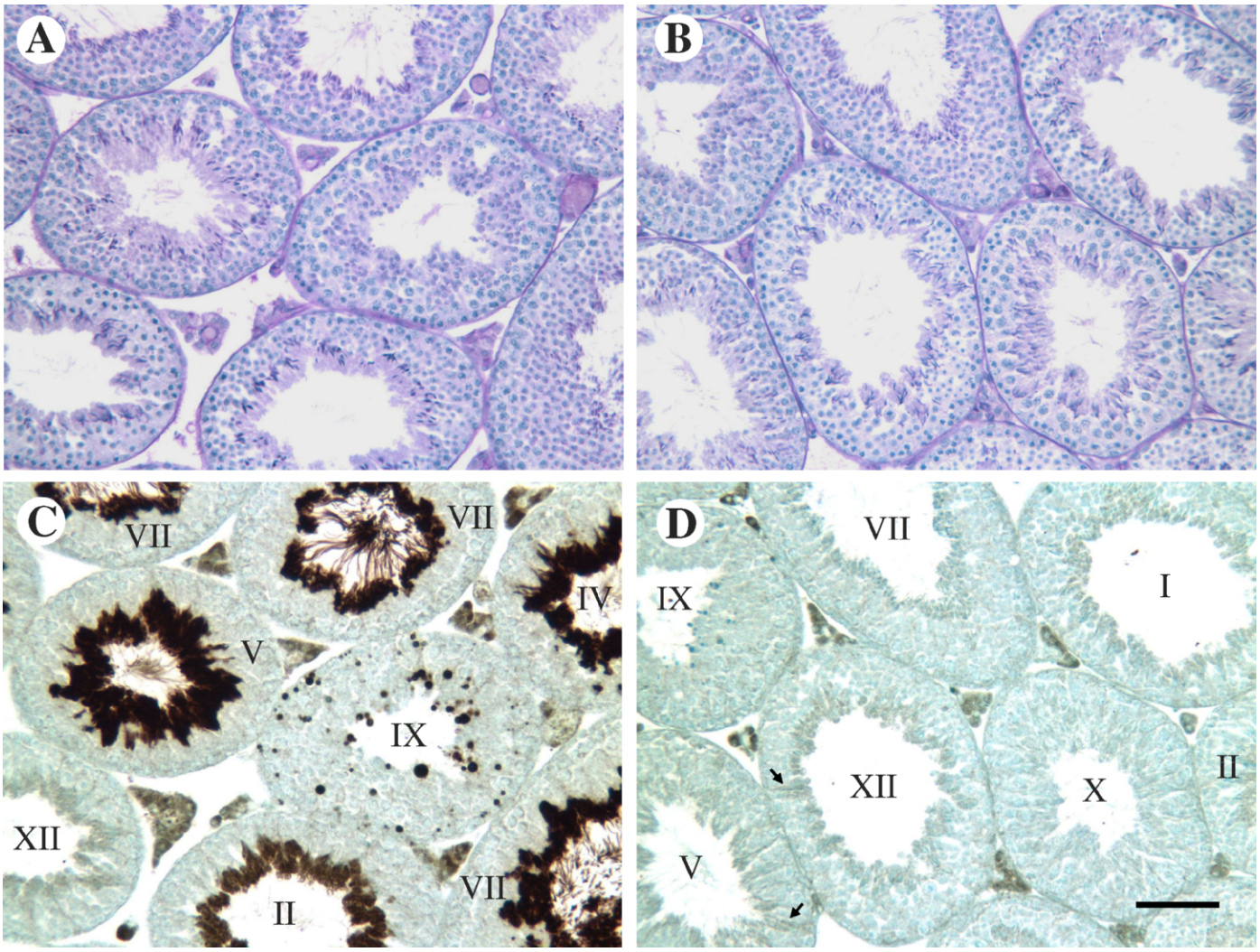

FIG. 3. Testis histology is not altered in *Pgk2*$^{-/-}$ mice. Adjacent testis sections from WT (**A**, **C**) and *Pgk2*$^{-/-}$ (**B**, **D**) were stained with periodic acid-Schiff and hematoxylin (**A**, **B**) or immunostained with PGK2 antiserum (antiserum 517; 1:2000) using the avidin-biotin immunoperoxidase procedure. Spermatogenesis and testis histology appear normal in *Pgk2*$^{-/-}$ males (**B**) and cannot be distinguished from WT males (**A**), despite the loss of intense PGK2 immunostaining in condensing spermatids (compare **D** with **C**). Roman numerals indicate the stages of the seminiferous cycle (**C**, **D**), and arrows (**D**) denote Sertoli cells with very faint staining that appears to result from cross-reactivity with PGK1. Bar in **D** = 50 μm.

group, the *Pgk2*$^{-/-}$ males sired a mean of 2.0 ± 1.1 pups during the 3-mo mating trial with two females per male. By comparison, *Pgk2*$^{+/-}$ males (n = 7) sired a mean of 29.6 ± 2.9 pups during the same time period when mated with a single female (either *Pgk2*$^{+/-}$ or C57BL/6NCrl). Heterozygous pairs produced male and female offspring with the expected Mendelian ratio of genotypes. Female *Pgk2*$^{-/-}$ mice (n = 6) were also fertile, producing 1.0 ± 0.1 litters each month, with a mean of 6.4 ± 0.8 pups per litter.

Loss of PGK2 Does Not Alter Testis Histology, Sperm Counts, or Sperm Ultrastructure

Pgk2$^{-/-}$ and WT males did not exhibit differences in appearance or behavior and showed no significant differences in body weight or in the weights of reproductive organs, including testis, epididymis + vas deferens, and seminal vesicles (Table 1). Testis histology was indistinguishable between WT and *Pgk2*$^{-/-}$ mice (Fig. 3, A and B). When sections adjacent to those shown in Figure 3, A and B, were labeled with the same PGK2 antibody used for Western blot analysis (Fig. 2, A and B), intense immunostaining was present in late spermatids in WT mice (Fig. 3C) but not in *Pgk2*$^{-/-}$ mice (Fig. 3D). Immunoreactivity in WT condensing spermatids increased substantially between steps 12 (stage XII seminiferous tubule) and 14 (stage II and III tubules) of spermiogenesis. By steps 15 and 16 (stage IV–VIII tubules), spermatid flagella extending into the tubule lumen were intensely stained. PGK2 was also apparent in residual bodies remaining in stage IX tubules after the release of sperm during stage VIII. In testis sections from both WT and *Pgk2*$^{-/-}$ mice, apparent cross-reactivity with PGK1 was seen in Leydig cells in the interstitium and at very low levels in the seminiferous epithelium, particularly in Sertoli cells. No immunoreactivity was observed in control slides when the primary antibody was omitted (not shown).

Pgk2$^{-/-}$ and WT males produced comparable numbers of cauda epididymal sperm (Table 1). Since sperm from *Gapdhs*$^{-/-}$ mice displayed subtle differences in fibrous sheath ultrastructure [30], we examined sperm from *Pgk2*$^{-/-}$ and WT mice by

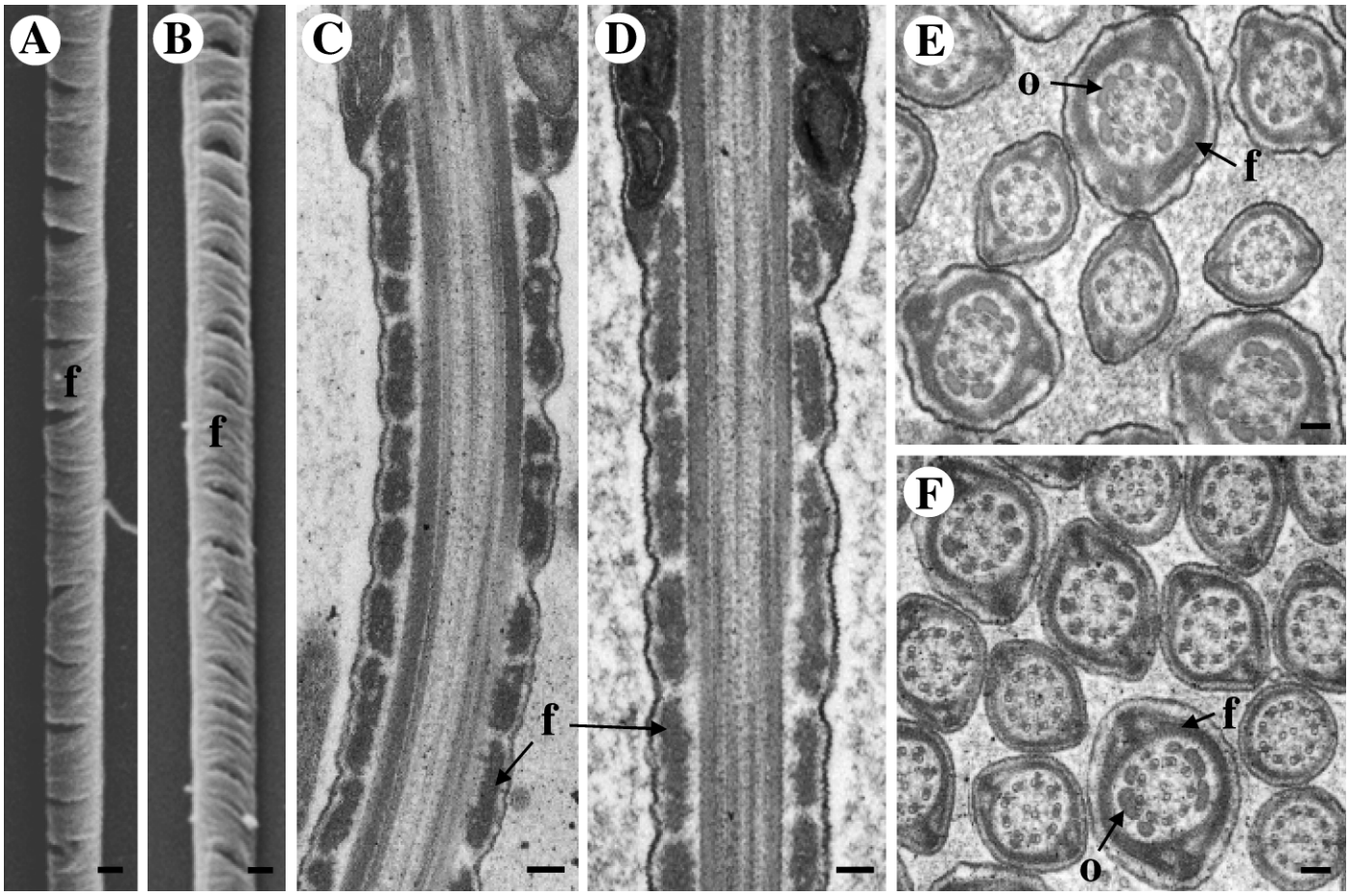

FIG. 4. Sperm ultrastructure appears normal in *Pgk2*$^{-/-}$ mice. Scanning (**A**, **B**) and transmission (**C**–**F**) electron micrographs did not detect differences between sperm from WT (**A**, **C**, and **E**) or *Pgk2*$^{-/-}$ (**B**, **D**, and **F**) males. Flagellar structures, including the fibrous sheath (f), outer dense fibers (o), and central axoneme, appear to be unaffected by the loss of PGK2. Bar = 0.2 μm (**A** and **B**) and 0.1 μm (**C**–**F**).

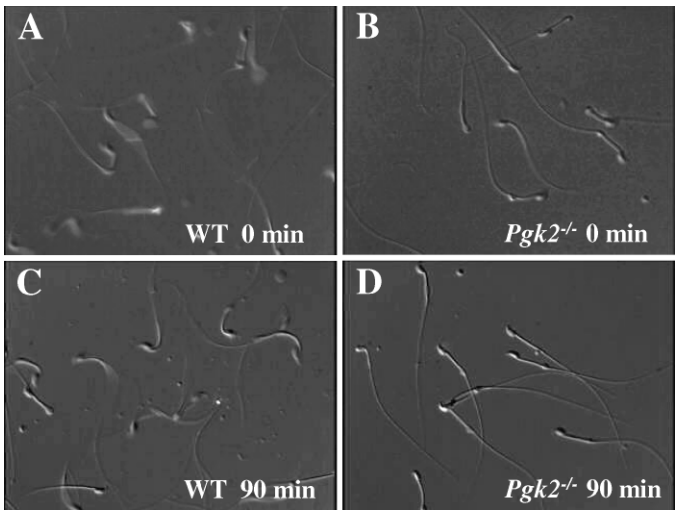

FIG. 5. Sperm motility is impaired in *Pgk2*$^{-/-}$ mice. Still images taken from supplemental movies (available online at www.biolreprod.org) are shown. Sperm from WT (**A**, **C**) and *Pgk2*$^{-/-}$ mice (**B**, **D**) were collected in M16 medium, and movies were recorded immediately after isolation (0 min; **A** and **B**; Supplemental Movies 1 and 2) and after incubation for 90 min at 37°C in an incubator with 5% CO_2 in air (**C** and **D**; Supplemental Movies 3 and 4). Original magnification ×250.

both scanning (Fig. 4, A and B) and transmission (Fig. 4, C–F) electron microscopy. These analyses focused on the principal piece of the flagellum where several glycolytic enzymes are localized [34]. The fibrous sheath, outer dense fibers, and central axoneme appeared normal in sperm lacking PGK2 (Fig. 4, B, D, and F). When the micrographs were not labeled with their genotypes, three experienced microscopists were unable to distinguish ultrastructural features of sperm from WT (Fig. 4, A, C, and E) and *Pgk2*$^{-/-}$ (Fig. 4, B, D, and F) mice.

PGK2 Is Required for Normal Sperm Motility

Sperm from *Pgk2*$^{-/-}$ mice exhibited marked defects in motility. Forward movement was observed immediately after isolation from the cauda epididymis, although the progression was substantially slower than for WT sperm (Fig. 5, A and B, and Supplemental Movies 1 and 2 available online at www.biolreprod.org). After incubating under capacitating conditions for 90 min in M16 medium, most sperm from *Pgk2*$^{-/-}$ males showed only nonprogressive, back-and-forth movement, whereas WT sperm retained vigorous motility (Fig. 5, C and D, and Supplemental Movies 3 and 4 available online at www.biolreprod.org). This nonprogressive pattern of movement was comparable to that seen for sperm from *Gapdhs*$^{-/-}$ mice just after collection from the cauda epididymis into M16 medium [30]. The images in Figure 5, B and D, also illustrate the normal appearance of sperm lacking PGK2.

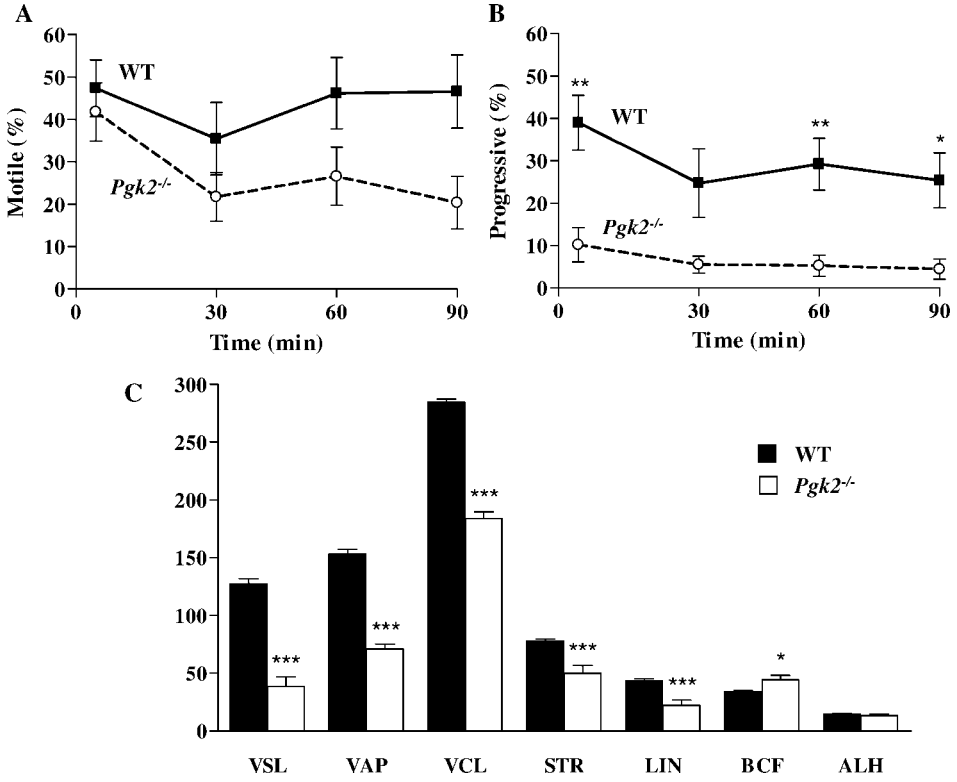

FIG. 6. Progressiveness and other quantitative parameters of motility are reduced in sperm lacking PGK2. Sperm from WT (n = 5) and *Pgk2*$^{-/-}$ (n = 5) mice were incubated in M16 medium for 90 min, and motility was assessed at 30-min intervals by CASA. Data are shown as mean values ± SEM. **A**) The mean percentage of motile PGK2-null sperm declined during the incubation, but was not significantly different from WT sperm. **B**) The mean percentage of progressive motility was significantly impaired in PGK2-null sperm, declining from 10.2% to 4.4% in 90 min. **C**) Immediately after isolation of sperm from the cauda epididymis, all CASA parameters of PGK2-null sperm (except ALH [amplitude of lateral head displacement]) were significantly different from WT sperm. VSL, straight line velocity (μm/sec); VAP, average path velocity (μm/sec); VCL, curvilinear velocity (μm/sec); STR, straightness; LIN, linearity; BCF, beat cross frequency (Hz). ***$P < 0.001$; **$P < 0.01$; *$P < 0.05$.

Quantitative parameters of sperm motility were assessed by CASA immediately after collection and at 30-min intervals during incubation in M16 (Fig. 6). The mean percentages of motile sperm from *Pgk2*$^{-/-}$ and WT mice were not statistically different at any time point, although the mean for PGK2-null sperm decreased to 20.4% by 90 min (Fig. 6A). Progressive motility (VAP > 80 μm/sec and STR > 50%) was more severely impaired in PGK2-null sperm (Fig. 6B). The mean percentage of progressive motility was initially only 10.2% for sperm from *Pgk2*$^{-/-}$ mice and subsequently declined to ≤5.5% between 30 and 90 min. Initial measurements related to velocity (VSL, VAP, and VCL) and progressiveness (VSL, VAP, STR, and LIN) were significantly lower for PGK2-null sperm compared to WT sperm ($P < 0.001$; Fig. 6C). Only BCF was higher for sperm lacking PGK2 ($P < 0.05$), and no difference between genotypes was seen for mean ALH. *Pgk2*-null sperm exhibited mostly nonprogressive tracks at subsequent time points (Fig. 6B), although sperm that were motile in these samples retained mean values for all CASA parameters that were not significantly different from the initial values.

ATP Levels Are Markedly Reduced in Sperm Lacking PGK2

We also monitored ATP levels of sperm incubated under capacitating conditions in M16 medium. Immediately after collection from the cauda epididymis, ATP levels for sperm from *Pgk2*$^{-/-}$ males were only 23% of those measured for WT sperm (Fig. 7A). ATP concentrations in PGK2-null sperm declined further to values <10% of WT levels within 30 min, while WT sperm maintained ATP production throughout the 90-min capacitation interval. At the initial time point, sperm from *Pgk2*$^{-/-}$ mice had consistently higher ATP levels than sperm from *Gapdhs*$^{-/-}$ mice ($P < 0.01$; Fig. 7B).

Sperm from WT and *Pgk2*$^{-/-}$ mice demonstrated similar rates of oxygen consumption when incubated in glucose-free M2 medium containing 0.33 mM pyruvate and 23.28 mM lactate, indicating comparable mitochondrial activity (Fig. 8). Oxygen consumption showed little change when dinitrophenol, EGTA, and succinate were added sequentially, indicating that sperm plasma membranes were intact (not shown). Maximal oxygen consumption, measured in digitonin-permeabilized sperm in the presence of succinate, was also comparable in WT and PGK2-null sperm (Fig. 8). These results indicate that reduced sperm motility and ATP levels in *Pgk2*$^{-/-}$ mice do not result from reduced activity of the mitochondrial respiratory chain.

Acylphosphatase May Contribute to Differences Between Sperm Lacking PGK2 or GAPDHS

We previously demonstrated that glyceraldehyde 3-phosphate, the GAPDHS substrate, was not metabolized in sperm from *Gapdhs*$^{-/-}$ mice and accumulated to levels 4-fold higher than in WT sperm [30]. However, we do not expect substrate accumulation in sperm from *Pgk2*$^{-/-}$ mice since 1,3-bisphosphoglycerate, the product of the GAPDHS reaction and substrate for PGK2, is highly unstable [45]. Furthermore, there are additional enzymes that can metabolize 1,3-bisphosphoglycerate. For example, acylphosphatase converts 1,3-bisphosphoglycerate to 3-phosphoglycerate, bypassing PGK2 and eliminating ATP production from this step in the glycolytic pathway (Fig. 9A). Both acylphosphatase isozymes, ACYP1 and ACYP2, were identified in a proteomic study of human sperm [46]. We assayed acylphosphatase activity and determined that the mean activity was 17 U/10^9 cells in sperm from WT and *Pgk2*$^{-/-}$ mice, more than three times higher than the activity in mouse erythrocytes (Fig. 9B). Although the acylphosphatase bypass of the PGK step of glycolysis would eliminate any net gain in ATP production from this pathway, it could provide downstream substrates for other pathways that influence ATP levels and motility in sperm from *Pgk2*$^{-/-}$ mice.

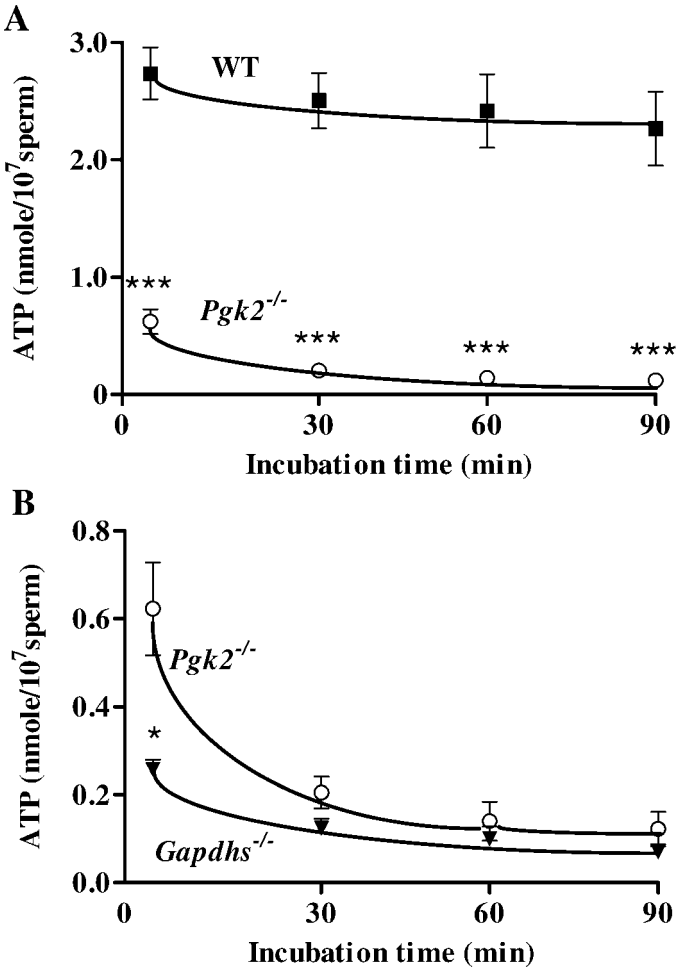

FIG. 7. Sperm ATP levels measured with a luciferase bioluminescence assay. **A**) ATP levels were significantly lower in sperm from *Pgk2*$^{-/-}$ mice (n = 15) compared to sperm from WT mice (n = 15) throughout a 90-min incubation period in M16 medium. **B**) Immediately after isolation from the cauda epididymis, however, sperm from *Pgk2*$^{-/-}$ mice had mean ATP levels that were >2-fold higher than levels in sperm from *Gapdhs*$^{-/-}$ mice (n = 5). Mean ATP levels ± SEM are shown. ***$P < 0.001$; *$P < 0.05$.

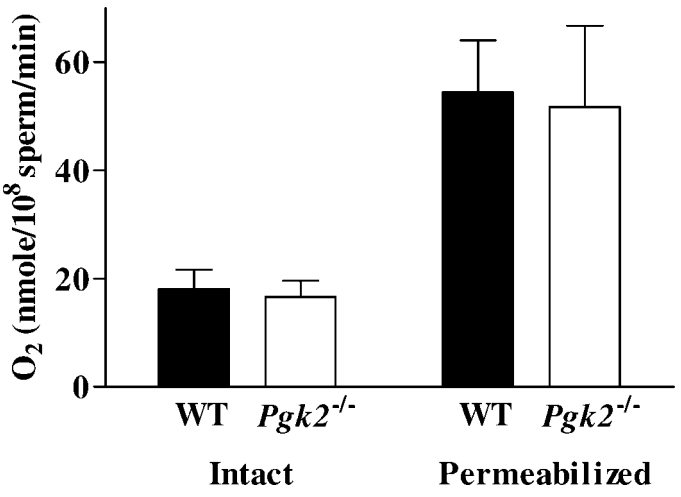

FIG. 8. Oxygen consumption was comparable for sperm from WT (n = 7) and *Pgk2*$^{-/-}$ mice (n = 5), both for intact sperm incubated in glucose-free medium and for permeabilized sperm incubated with succinate. Mean values ± SEM are shown and there was no statistical difference between genotypes.

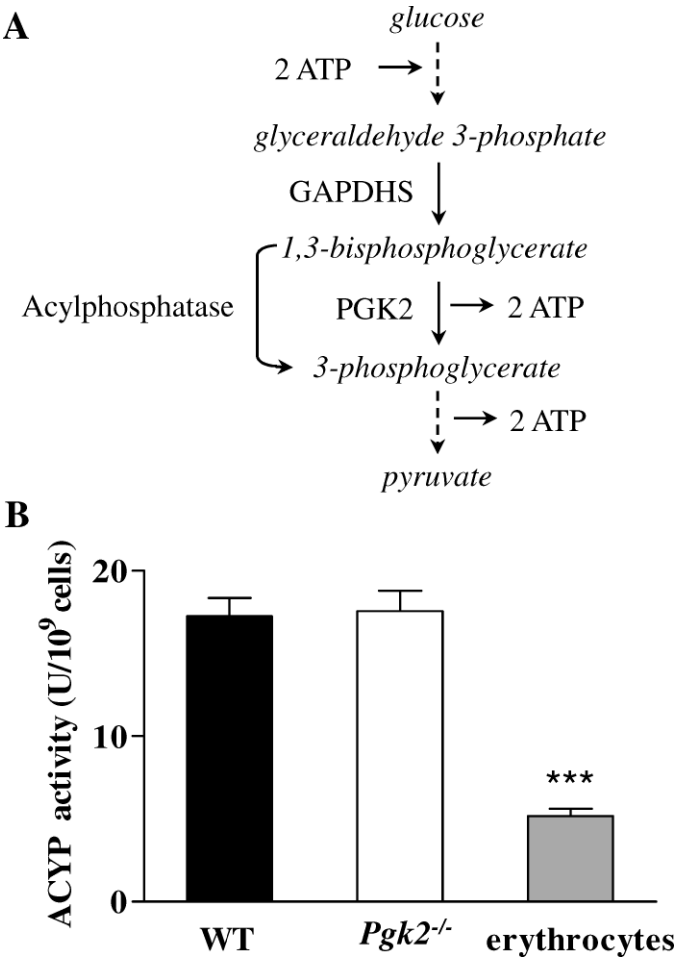

FIG. 9. Mouse sperm have acylphosphatase activity. **A**) Abbreviated diagram of glycolysis, showing a possible bypass of the PGK2 step by acylphosphatase. **B**) Mean acylphosphatase activities ± SEM are shown for sperm from WT mice (n = 6), sperm from *Pgk2*$^{-/-}$ mice (n = 3), and erythrocytes from C57BL/6NCrl mice (n = 3). ***$P < 0.001$.

DISCUSSION

The *Pgk2* retrogene is highly conserved in mammals and has been proposed to compensate for the loss of *Pgk1* expression during spermatogenesis due to meiotic sex chromosome inactivation [5]. However, targeted deletion of *Pgk2* does not alter testis histology, sperm counts, or sperm ultrastructure, indicating that this isozyme is not required for the completion of spermatogenesis. Although it is possible that very low levels of PGK1 retained after meiosis [10, 33] are sufficient for spermatid metabolism, our results support the conclusion of earlier in vitro studies that glycolysis is not required during the haploid period. Isolated rodent spermatids use lactate preferentially and undergo rapid ATP depletion and cell death when glucose is the sole energy substrate [47–50]. The accumulation of fructose 1,6-bisphosphate and triose phosphates, but not downstream metabolic intermediates, suggests that glycolysis is limited in round spermatids by inhibition of GAPDH [47, 48]. Glycolysis has not been examined during the later stages of spermiogenesis (steps 9–16 in the mouse) when several germ cell-specific isozymes are synthesized and assembled in association with the fibrous sheath in the developing sperm flagellum [15, 18, 34].

Our immunohistochemical analyses detected PGK2 in the principal piece of the sperm flagellum during steps 15 and 16 of spermiogenesis. However, we were unable to determine if PGK2 is localized exclusively in the principal piece, because our antibodies proved unsuitable for labeling isolated sperm with immunofluorescent or immunocytochemical methods. Partial retention of PGK2 during sonication and sequential extraction of sperm tails with 1% Triton X-100 and 0.6 M KSCN [34] suggests that this sperm isozyme may interact with other glycolytic enzymes or components of the fibrous sheath. Unlike GAPDHS and sperm-specific aldolase isozymes that are tightly bound to the fibrous sheath [15, 18], PGK2 does not have a distinct N-terminal extension available for interactions with sperm cytoskeletal constituents. However, structural analyses indicate that PGK2 amino acids with significant chemical differences from PGK1 are clustered in a C-terminal domain where they could mediate protein interactions without hindering catalysis [33, 51].

Defects in sperm metabolism and motility appear to be primarily responsible for male infertility in mice that lack PGK2. Therefore, *Pgk2* compensation for *Pgk1* is required for sperm function rather than sperm formation. In addition to providing further evidence for the key role of glycolytic ATP production in sperm, this study identified unexpected phenotypic differences between sperm that lack either GAPDHS [30] or PGK2. These enzymes catalyze successive steps in glycolysis, and loss of either one should eliminate ATP production via this pathway (Fig. 9A). However, sperm lacking PGK2 had higher ATP levels immediately after isolation from the cauda epididymis compared to sperm lacking GAPDHS and exhibited higher percentages of progressive motility throughout 90-min incubations in M16 medium. Although mean progressive motility (VAP $>$ 80 μm/sec and STR $>$ 50%) declined from 10.2% to 4.4% during this interval, the retention of a small number of progressive sperm probably accounts for the occasional pups sired by $Pgk2^{-/-}$ males. In contrast, $Gapdhs^{-/-}$ males were completely infertile and produced sperm with mean progressive motility that did not exceed 0.3% immediately after collection in M16 medium and dropped to 0% within 30 min [30].

The phenotypic differences between $Gapdhs^{-/-}$ and $Pgk2^{-/-}$ mice led us to examine alternative pathways that branch from glycolysis at the level of these two enzymes. One pathway that bypasses the PGK step of glycolysis is the Rapoport-Luebering shunt, which functions in erythrocytes to produce 2,3-bisphosphoglycerate, a regulator of hemoglobin oxygen affinity [52]. 2,3-Bisphosphoglycerate mutase (BPGM) catalyzes this two-step reaction, using synthase activity to convert 1,3-bisphosphoglycerate to 2,3-bisphosphoglycerate and phosphatase activity to convert 2,3-bisphosphoglycerate to 3-phosphoglycerate [53]. BPGM is frequently considered an erythrocyte-specific enzyme. It was recently reported that this enzyme is also expressed in the syncytiotrophoblast layer of the human placenta, where it may facilitate oxygen transfer between maternal and fetal hemoglobin [54]. It is interesting to note that microarray analyses also detected BPGM mRNA in mouse pachytene spermatocytes and round spermatids (http://mrg.genetics.washington.edu/) [55]. We have not yet examined this pathway since there are no reports of BPGM in sperm.

A similar bypass of the PGK step of glycolysis is catalyzed by acylphosphatase (Fig. 9A), a cytosolic enzyme that hydrolyzes 1,3-bisphosphoglycerate and other acylphosphates with a carboxylphosphate bond [56]. There are two acylphosphatase isozymes, ACYP1 (erythrocyte or common type) and ACYP2 (muscle type), and both have been identified in human sperm with proteomics methods [46]. In this study we determined that acylphosphatase activity is also present in mouse sperm. It is likely that ACYP1 accounts for most of this activity since *Acyp1* mRNA levels are high in pachytene spermatocytes and round spermatids, while *Acyp2* transcripts are barely detectable throughout spermatogenesis in the mouse (http://mrg.genetics.washington.edu/) [55]. The acylphosphatases hydrolyze intermediates in multiple metabolic pathways and have been proposed to regulate both glycolysis and cation transport via membrane ATPases [56, 57].

The presence of acylphosphatase or other enzymes that bypass the PGK step of glycolysis may reduce the accumulation of glycolytic intermediates in sperm that lack PGK2 and provide downstream substrates that can be metabolized by other pathways. We are currently using NMR-based metabolomic analyses to compare metabolites produced in sperm from $Gapdhs^{-/-}$, $Pgk2^{-/-}$, and WT mice. In our initial experiments, multiple metabolites that are elevated in sperm from both knockouts are significantly higher in sperm lacking GAPDHS compared to sperm lacking PGK2. We anticipate that these analyses will provide further insights into the metabolic requirements for optimal sperm function. Comparative analyses of sperm maturation and capacitation in $Pgk2^{-/-}$ and $Gapdhs^{-/-}$ mice should also improve our understanding of the metabolism-dependent signaling events required for fertilization.

ACKNOWLEDGMENTS

We thank several of our colleagues for valuable assistance with these studies, including Ms. Victoria Madden and Dr. C. Robert Bagnell in the UNC Microscopy Services Core for scanning and transmission electron microscopy, Ms. Gail Grossman in the Molecular Histology Core for immunohistochemistry, Dr. Ekhson Holmuhamedov for oxygen consumption measurements, and Ms. Shannon Toffton and Ms. Rebecca Jo for mouse colony maintenance.

REFERENCES

1. McCarrey JR, Berg WM, Paragioudakis SJ, Zhang PL, Dilworth DD, Arnold BL, Rossi JJ. Differential transcription of Pgk genes during spermatogenesis in the mouse. Dev Biol 1992; 154:160–168.
2. Yoshioka H, Geyer CB, Hornecker JL, Patel KT, McCarrey JR. In vivo analysis of developmentally and evolutionarily dynamic protein-DNA interactions regulating transcription of the Pgk2 gene during mammalian spermatogenesis. Mol Cell Biol 2007; 27:7871–7885.
3. Turner JM. Meiotic sex chromosome inactivation. Development 2007; 134:1823–1831.
4. Namekawa SH, Park PJ, Zhang LF, Shima JE, McCarrey JR, Griswold MD, Lee JT. Postmeiotic sex chromatin in the male germline of mice. Curr Biol 2006; 16:660–667.
5. McCarrey JR, Thomas K. Human testis-specific PGK gene lacks introns and possesses characteristics of a processed gene. Nature 1987; 326:501–505.
6. Boer PH, Adra CN, Lau YF, McBurney MW. The testis-specific phosphoglycerate kinase gene pgk-2 is a recruited retroposon. Mol Cell Biol 1987; 7:3107–3112.
7. VandeBerg JL, Cooper DW, Close PJ. Testis specific phosphoglycerate kinase B in mouse. J Exp Zool 1976; 198:231–240.
8. Gold B, Fujimoto H, Kramer JM, Erickson RP, Hecht NB. Haploid accumulation and translational control of phosphoglycerate kinase-2 messenger RNA during mouse spermatogenesis. Dev Biol 1983; 98: 392–399.
9. Iguchi N, Tobias JW, Hecht NB. Expression profiling reveals meiotic male germ cell mRNAs that are translationally up- and down-regulated. Proc Natl Acad Sci U S A 2006; 103:7712–7717.
10. Kramer JM, Erickson RP. Developmental program of PGK-1 and PGK-2 isozymes in spermatogenic cells of the mouse: specific activities and rates of synthesis. Dev Biol 1981; 87:37–45.
11. Bluthmann H, Cicurel L, Kuntz GW, Haedenkamp G, Illmensee K. Immunohistochemical localization of mouse testis-specific phosphoglycerate kinase (PGK-2) by monoclonal antibodies. EMBO J 1982; 1:479–484.
12. Kramer JM. Immunofluorescent localization of PGK-1 and PGK-2

isozymes within specific cells of the mouse testis. Dev Biol 1981; 87:30–36.
13. Vandeberg JL, Lee CY, Goldberg E. Immunohistochemical localization of phosphoglycerate kinase isozymes in mouse testes. J Exp Zool 1981; 217: 435–441.
14. Welch JE, Schatte EC, O'Brien DA, Eddy EM. Expression of a glyceraldehyde 3-phosphate dehydrogenase gene specific to mouse spermatogenic cells. Biol Reprod 1992; 46:869–878.
15. Bunch DO, Welch JE, Magyar PL, Eddy EM, O'Brien DA. Glyceraldehyde 3-phosphate dehydrogenase-S protein distribution during mouse spermatogenesis. Biol Reprod 1998; 58:834–841.
16. Goldberg E. Lactic and malic dehydrogenases in human spermatozoa. Science 1963; 139:602–603.
17. Li SS, O'Brien DA, Hou EW, Versola J, Rockett DL, Eddy EM. Differential activity and synthesis of lactate dehydrogenase isozymes A (muscle), B (heart), and C (testis) in mouse spermatogenic cells. Biol Reprod 1989; 40:173–180.
18. Vemuganti SA, Bell TA, Scarlett CO, Parker CE, de Villena FP, O'Brien DA. Three male germline-specific aldolase A isozymes are generated by alternative splicing and retrotransposition. Dev Biol 2007; 309:18–31.
19. Mori C, Welch JE, Fulcher KD, O'Brien DA, Eddy EM. Unique hexokinase messenger ribonucleic acids lacking the porin-binding domain are developmentally expressed in mouse spermatogenic cells. Biol Reprod 1993; 49:191–203.
20. Mori C, Nakamura N, Welch JE, Gotoh H, Goulding EH, Fujioka M, Eddy EM. Mouse spermatogenic cell-specific type 1 hexokinase (mHk1-s) transcripts are expressed by alternative splicing from the mHk1 gene and the HK1-S protein is localized mainly in the sperm tail. Mol Reprod Dev 1998; 49:374–385.
21. Eddy EM, Toshimori K, O'Brien DA. Fibrous sheath of mammalian spermatozoa. Microsc Res Tech 2003; 61:103–115.
22. Mukai C, Okuno M. Glycolysis plays a major role for adenosine triphosphate supplementation in mouse sperm flagellar movement. Biol Reprod 2004; 71:540–547.
23. Peterson RN, Freund M. ATP synthesis and oxidative metabolism in human spermatozoa. Biol Reprod 1970; 3:47–54.
24. Williams AC, Ford WC. The role of glucose in supporting motility and capacitation in human spermatozoa. J Androl 2001; 22:680–695.
25. Travis AJ, Jorgez CJ, Merdiushev T, Jones BH, Dess DM, Diaz-Cueto L, Storey BT, Kopf GS, Moss SB. Functional relationships between capacitation-dependent cell signaling and compartmentalized metabolic pathways in murine spermatozoa. J Biol Chem 2001; 276:7630–7636.
26. Urner F, Leppens-Luisier G, Sakkas D. Protein tyrosine phosphorylation in sperm during gamete interaction in the mouse: the influence of glucose. Biol Reprod 2001; 64:1350–1357.
27. Fraser LR, Quinn PJ. A glycolytic product is obligatory for initiation of the sperm acrosome reaction and whiplash motility required for fertilization in the mouse. J Reprod Fertil 1981; 61:25–35.
28. Cooper TG. The onset and maintenance of hyperactivated motility of spermatozoa in the mouse. Gamete Res 1984; 9:55–74.
29. Hoshi K, Tsukikawa S, Sato A. Importance of Ca2+, K+ and glucose in the medium for sperm penetration through the human zona pellucida. Tohoku J Exp Med 1991; 165:99–104.
30. Miki K, Qu W, Goulding EH, Willis WD, Bunch DO, Strader LF, Perreault SD, Eddy EM, O'Brien DA. Glyceraldehyde 3-phosphate dehydrogenase-S, a sperm-specific glycolytic enzyme, is required for sperm motility and male fertility. Proc Natl Acad Sci U S A 2004; 101: 16501–16506.
31. Odet F, Duan C, Willis WD, Goulding EH, Kung A, Eddy EM, Goldberg E. Expression of the gene for mouse lactate dehydrogenase C (Ldhc) is required for male fertility. Biol Reprod 2008; 79:26–34.
32. Narisawa S, Hecht NB, Goldberg E, Boatright KM, Reed JC, Millan JL. Testis-specific cytochrome c-null mice produce functional sperm but undergo early testicular atrophy. Mol Cell Biol 2002; 22:5554–5562.
33. McCarrey JR, Kumari M, Aivaliotis MJ, Wang Z, Zhang P, Marshall F, Vandeberg JL. Analysis of the cDNA and encoded protein of the human testis-specific PGK-2 gene. Dev Genet 1996; 19:321–332.
34. Krisfalusi M, Miki K, Magyar PL, O'Brien DA. Multiple glycolytic enzymes are tightly bound to the fibrous sheath of mouse spermatozoa. Biol Reprod 2006; 75:270–278.
35. Osoegawa K, Tateno M, Woon PY, Frengen E, Mammoser AG, Catanese JJ, Hayashizaki Y, de Jong PJ. Bacterial artificial chromosome libraries for mouse sequencing and functional analysis. Genome Res 2000; 10:116–128.
36. Dix DJ, Allen JW, Collins BW, Mori C, Nakamura N, Poorman-Allen P, Goulding EH, Eddy EM. Targeted gene disruption of Hsp70–2 results in failed meiosis, germ cell apoptosis, and male infertility. Proc Natl Acad Sci U S A 1996; 93:3264–3268.
37. Leblond CP, Clermont Y. Spermiogenesis of rat, mouse, hamster and guinea pig as revealed by the periodic acid-fuchsin sulfurous acid technique. Am J Anat 1952; 90:167–215.
38. Russell LD, Ettlin RA, Sinha Hikim AP, Clegg ED. Histological and Histopathological Evaluation of the Testis. Clearwater, FL: Cache River Press; 1990.
39. Miki K, Willis WD, Brown PR, Goulding EH, Fulcher KD, Eddy EM. Targeted disruption of the Akap4 gene causes defects in sperm flagellum and motility. Dev Biol 2002; 248:331–342.
40. Fokina KV, Dainyak MB, Nagradova NK, Muronetz VI. A study on the complexes between human erythrocyte enzymes participating in the conversions of 1,3-diphosphoglycerate. Arch Biochem Biophys 1997; 345:185–192.
41. Ramponi G, Treves C, Guerritore AA. Aromatic acyl phosphates as substrates of acyl phosphatase. Arch Biochem Biophys 1966; 115:129–135.
42. Camici G, Manao G, Cappugi G, Ramponi G. A new synthesis of benzoyl phosphate: a substrate for acyl phosphatase assay. Experientia 1976; 32: 535–536.
43. Holmuhamedov EL, Jovanovic S, Dzeja PP, Jovanovic A, Terzic A. Mitochondrial ATP-sensitive K+ channels modulate cardiac mitochondrial function. Am J Physiol 1998; 275:H1567–H1576.
44. Becker GL, Fiskum G, Lehninger AL. Regulation of free Ca2+ by liver mitochondria and endoplasmic reticulum. J Biol Chem 1980; 255:9009–9012.
45. Krimsky I. Enzymatic formation of high levels of 1,3-diphosphoglycerate from 3-phosphoglycerate: isolation and further metabolism. J Biol Chem 1959; 234:228–231.
46. Martinez-Heredia J, Estanyol JM, Ballesca JL, Oliva R. Proteomic identification of human sperm proteins. Proteomics 2006; 6:4356–4369.
47. Nakamura M, Fujiwara A, Yasumasu I, Okinaga S, Arai K. Regulation of glucose metabolism by adenine nucleotides in round spermatids from rat testes. J Biol Chem 1982; 257:13945–13950.
48. Nakamura M, Okinaga S, Arai K. Studies of metabolism of round spermatids: glucose as unfavorable substrate. Biol Reprod 1986; 35: 927–935.
49. Grootegoed JA, Jansen R, van der Molen HJ. Effect of glucose on ATP dephosphorylation in rat spermatids. J Reprod Fertil 1986; 77:99–107.
50. Grootegoed JA, Mackenbach P, Oonk RB. Sertoli cell-germ cell interactions in the regulation of spermatogenesis. In: Parvinen M, Huhtaniemi I, Pelliniemi LJ (eds.), Development and Function of the Reproductive Organs. Rome: Ares-Serono Symposia; 1988:91–101.
51. Sawyer GM, Monzingo AF, Poteet EC, O'Brien DA, Robertus JD. X-ray analysis of phosphoglycerate kinase 2, a sperm-specific isoform from *Mus musculus*. Proteins 2008; 71:1134–1144.
52. van Wijk R, van Solinge WW. The energy-less red blood cell is lost: erythrocyte enzyme abnormalities of glycolysis. Blood 2005; 106:4034–4042.
53. Wang Y, Wei Z, Bian Q, Cheng Z, Wan M, Liu L, Gong W. Crystal structure of human bisphosphoglycerate mutase. J Biol Chem 2004; 279: 39132–39138.
54. Pritlove DC, Gu M, Boyd CA, Randeva HS, Vatish M. Novel placental expression of 2,3-bisphosphoglycerate mutase. Placenta 2006; 27: 924–927.
55. Shima JE, McLean DJ, McCarrey JR, Griswold MD. The murine testicular transcriptome: characterizing gene expression in the testis during the progression of spermatogenesis. Biol Reprod 2004; 71:319–330.
56. Stefani M, Taddei N, Ramponi G. Insights into acylphosphatase structure and catalytic mechanism. Cell Mol Life Sci 1997; 53:141–151.
57. Thunnissen MM, Taddei N, Liguri G, Ramponi G, Nordlund P. Crystal structure of common type acylphosphatase from bovine testis. Structure 1997; 5:69–79.